The glutathione conjugate of ethacrynic acid can bind to human pi class glutathione transferase P1-1 in two different modes

Aaron J. Oakley[a], Mario Lo Bello[b], Anna Paola Mazzetti[b], Giorgio Federici[c], Michael W. Parker[a,*]

[a] *The Ian Potter Foundation Protein Crystallography Laboratory, St. Vincent's Institute of Medical Research, 41 Victoria Parade, Fitzroy, Vic. 3065, Australia*
[b] *Department of Biology, University of Rome 'Tor Vergata', Via della Ricerca Scientifica, 00133 Rome, Italy*
[c] *Ospedale Pediatrico IRCCS 'Bambin Gesù', 00165 Rome, Italy*

Received 29 September 1997; revised version received 3 November 1997

Abstract The diuretic drug ethacrynic acid, an inhibitor of pi class glutathione *S*-transferase, has been tested in clinical trials as an adjuvant in chemotherapy. We recently solved the crystal structure of this enzyme in complex with ethacrynic acid and its glutathione conjugate. Here we present a new structure of the ethacrynic-glutathione conjugate complex. In this structure the ethacrynic moiety of the complex is shown to bind in a completely different orientation to that previously observed. Thus there are at least two binding modes possible, an observation of great importance to the design of second generation inhibitors of the enzyme.

Key words: Drug design; Ethacrynic acid; Enzyme-inhibitor complex; Glutathione transferase; X-ray structure; Human

1. Introduction

The glutathione *S*-transferases (GSTs, EC 2.5.1.18) are a family of enzymes that conjugate electrophilic substrates to the tripeptide glutathione (GSH, γ-Glu-Cys-Gly). GSTs have been used as markers for malignant tumours and have been implicated in the development of resistance of tumours towards various anti-cancer drugs [1–4]. The pi class isoform of GSTs, in particular, has been implicated in resistance and there are currently major efforts to find specific inhibitors of this isoform to be used as adjuvants in chemotherapy [4]. The diuretic drug ethacrynic acid (EA, [2,3-dichloro-4-(2-methylenebutyryl)-phenoxy]acetic acid, see Fig. 1) is an inhibitor of pi class GSTs [5]. A number of investigators have explored the possibility of inhibiting GSTs with EA as a means of overcoming acquired multi-drug resistance [6–8]. In a recent study, EA was administered in conjunction with thiotepa to 27 previously treated patients with advanced cancer [9]. Pi class GST activity was reduced and the tumours were found to have increased sensitivity to thiotepa. However, EA was found to cause side-effects that proved too severe to continue with phase II trials of the inhibitor.

EA is a known inhibitor of GSTs but in addition can act as a substrate. EA is thought to form a conjugate with GSH via Michael addition, both spontaneously and by GST-driven catalysis [5,10,11]. The α,β-unsaturated ketone moiety (Fig. 1) is the target for conjugation by GSH [11]. The reaction of the pi class GST with EA is often considered a characteristic feature of this isoenzyme [12]. The EA-GSH conjugate also acts as an inhibitor. In the case of human pi class GST the EA-GSH conjugate is a more potent inhibitor than the parent compound ($K_i = 1.5$ vs 11.5 μM, respectively) [11].

The first structures of a GST complexed with EA and its glutathione conjugate were determined by Cameron and coworkers [13] who crystallised the complexes in the presence of the human alpha class enzyme. Although the alpha class enzyme possesses the canonical GST fold, it shares only 32% sequence identity with the pi class enzyme and has a C-terminal extension that folds into part of the active site. We recently solved the crystal structure of human pi class GST P1-1 in complex with the same inhibitors [14]. We have since discovered that the glutathione conjugate of EA can bind in an alternative mode to the one that was recently described. Here we present the new structure and discuss it in the light of the previously published results. The difference in the two structures can be ascribed to different crystallisation conditions: in the published structure, the inhibitor was soaked into preformed crystals whereas in the structure reported here, the complex was formed by cocrystallisation. The binding of EA-GSH in two different modes to the enzyme has implications for the design of second generation inhibitors of the enzyme.

2. Material and methods

2.1. Crystallisation and data collection

Crystallisation was performed by the hanging drop vapour diffusion method using 24-well tissue culture plates. A 2 μl droplet of an 8 mg/ml protein solution containing 10 mM phosphate buffer (pH 7.0), 1 mM EDTA and 2 mM mercaptoethanol was mixed with equal volumes of a saturated solution of EA-GSH in 0.14% Triton X-100 and reservoir solution. The EA-GSH was synthesised according to Ploemen and coworkers [5]. The drop was applied to a siliconised coverslip which was sealed to the top of the well with vacuum grease. Each well contained 1 ml of reservoir solution. The reservoir solution consisted of 25% (w/v) ammonium sulphate, 30–60 mM DTT, 100 mM MES buffer (pH range 6.2–6.4) and 5% (v/v) glycerol. The trials were carried out at a constant temperature of 22°C. The drops were allowed to equilibrate for 1 day before they were streak-seeded with a cat's whisker from drops containing crystals grown under similar conditions. Crystals appeared in the shape of plates after 1 week and grew to maximal dimensions of 0.1 mm × 0.3 mm × 0.3 mm. The complex crystallised in the space group C2 with cell dimensions $a = 77.8$ Å, $b = 89.6$ Å, $c = 68.7$ Å and $\beta = 97.6°$.

The X-ray diffraction data were collected using a MARResearch area detector with CuK_α X-rays generated by a Rigaku RU-200 rotating anode X-ray generator. The data were collected at 100 K using an Oxford Cryosystems Cryostream Cooler. Prior to flash-freezing, the crystal was transferred to artificial mother liquor containing 20% glycerol. The diffraction data were processed and analysed using

*Corresponding author. Fax: (61) (3) 9416-2676.
E-mail: mwp@rubens.its.unimelb.edu.au

PII S0014-5793(97)01424-5

programs in the HKL [15] and CCP4 suites [16]. A data set off the one frozen crystal was collected to 2.3 Å resolution with 84.3% completeness (17 514 unique reflections), an I/σ_I of 6.5 and a R_{sym} of 13.0%. In the highest resolution bin, 2.35–2.30 Å, the completeness was 90.7%, the I/σ_I was 3.5 and the R_{sym} was 23.9%.

2.2. Structure solution and refinement

The starting model for refinement was the refined *S*-hexyl GSH complex model as observed in the C2 space group (*R*-factor = 20.0% and R_{free} = 24.5% for resolution limits 6.0–1.95 Å; unpublished results). All water molecules and the *S*-hexyl GSH inhibitor were omitted prior to use. Rigid body refinement in XPLOR version 3.1 [17] was used to compensate for any possible changes in crystal packing. As the asymmetric unit of the crystal contained two GST monomers, use was made of the non-crystallographic symmetry restraints on all non-hydrogen atoms throughout the course of refinement. The starting model gave an *R*-factor of 37.4% (R_{free} = 40.0%) which reduced to 34.0% (R_{free} = 35.8%) after rigid body refinement. The model was then subjected to two cycles of positional and isotropically restrained individual *B*-factor refinement and inclusion of water and MES buffer molecules (*R*-factor = 23.8%, R_{free} = 30.1%). The $2F_{inhibitor}-F_{native}$ electron density map calculated from this model was further improved by 10 cycles of twofold non-crystallographic averaging using MAMA [18], RAVE [18] and CCP4 [16] program suites. The averaged electron density maps allowed unambiguous placement of the inhibitor (Fig. 2). The density for the chlorine atoms of the inhibitor was very clear. If the atoms at the chlorine positions were given scattering factors for carbon in the Fourier calculations, two strong peaks were positioned over both atoms confirming the identification of the chlorine atoms. The conjugation of GSH with EA can theoretically result in two possible diastereomers. After appropriate rotation of torsion angles so that each diastereomer would fit the electron density, the only significant difference between the two molecules is the positioning of the C9 and C11 atoms of the ethyl group (see Fig. 3). The difference in positioning of these atoms is less than 0.6 Å and is not distinguishable in the electron density maps. Because the electron density is broken over these atoms (Fig. 2), it is likely there is an approximately equal mixture of the two diastereomers. We have chosen only one diastereomer for simplicity. Bond lengths and angles for the inhibitor were derived from a model built and energy-minimised using programs in the INSIGHT II software suite (Molecular Simulations Inc., San Diego, CA, USA). The model was then subjected to a round of positional refinement (*R*-factor = 23.3%, R_{free} = 29.2%). After two more rounds of refinement and rebuilding, the model yielded an *R*-factor of 21.9% (R_{free} = 28.1%). The temperature factors of the inhibitor were set to that of the surrounded side-chains and the inhibitor occupancies refined. The values obtained were 0.60 for the A monomer and 0.58 for the B monomer. After application of a bulk solvent correction the final *R*-factor was 21.4% (R_{free} = 27.0%) for all data between 15.0 Å and 2.3 Å resolution. The root-mean-square (rms) deviations from ideal bond lengths and bond angles are 0.009 Å and 1.3°, respectively. The final model consists of 3262 non-hydrogen protein atoms, 78 inhibitor atoms, 24 atoms corresponding to two MES buffer molecules and 174 water molecules. The fit of the inhibitor to the final electron density map is shown in Fig. 2. A stereochemical analysis of the refined structure with the program PROCHECK [19] gave values either similar to or better than expected for structures refined at similar resolutions.

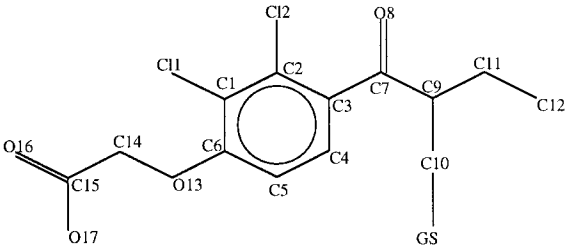

Fig. 1. Schematic representation of EA-GSH. The numbering scheme is taken from Lamotte and coworkers [22].

3. Results and discussion

The human pi class GST is a homodimer with 209 residues per monomer. The structure was originally determined from crystals of the enzyme complexed to the inhibitor, *S*-hexyl GSH [20]. Each monomer was shown to consist of two domains: the N-terminal domain (residues 1–76) and the C-terminal domain (residues 83–209). The GSH binding site, or G site, was located in a cleft formed between the two domains and most of the residues contacting GSH are provided by residues from the N-terminal domain (Figs. 3 and 4). The binding site for the hydrophobic electrophile, or H site, was located immediately adjacent to the G site and formed part of the solvent-exposed cleft between the two domains. Residues in the H site are provided by both domains.

The crystal structures of the human pi class GST complexed to EA and EA-GSH have recently been published [14]. The models were refined to 1.9 Å resolution with crystallographic *R*-factors of 21.0% and 20.6% respectively. In the EA complex, the inhibitor was found in a similar position to that of the hexyl moiety of the previously determined *S*-hexyl GSH complex crystal structure [20] (Figs. 3 and 5). The aromatic ring of the inhibitor was stacked between the aromatic side chains of Phe^{8} and Tyr^{108} and the inhibitor formed, in total, 38 van der Waals interactions with the protein. In the EA-GSH complex, the GSH moiety was found to bind to

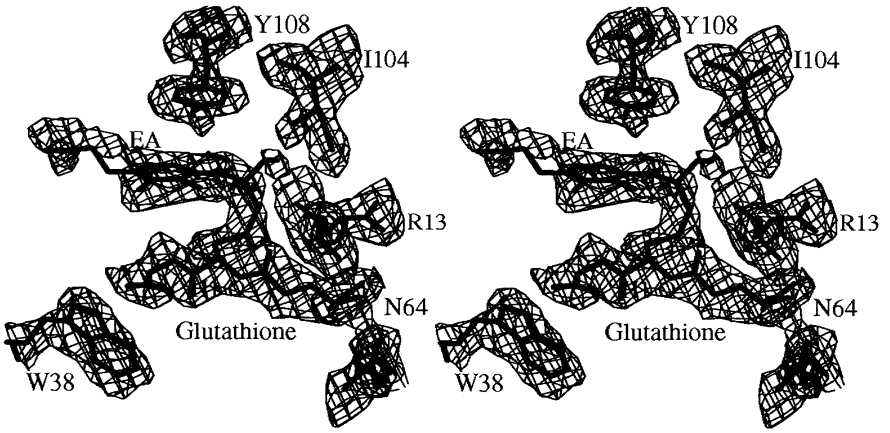

Fig. 2. Stereo diagram of the final $2F_{inhibitor}-F_{calc}$ electron density map of the EA-GSH complex in the vicinity of the inhibitor binding site of human GST P1-1. The map was calculated using all reflections between 40.0 Å and 2.3 Å and contoured at the 0.7σ level.

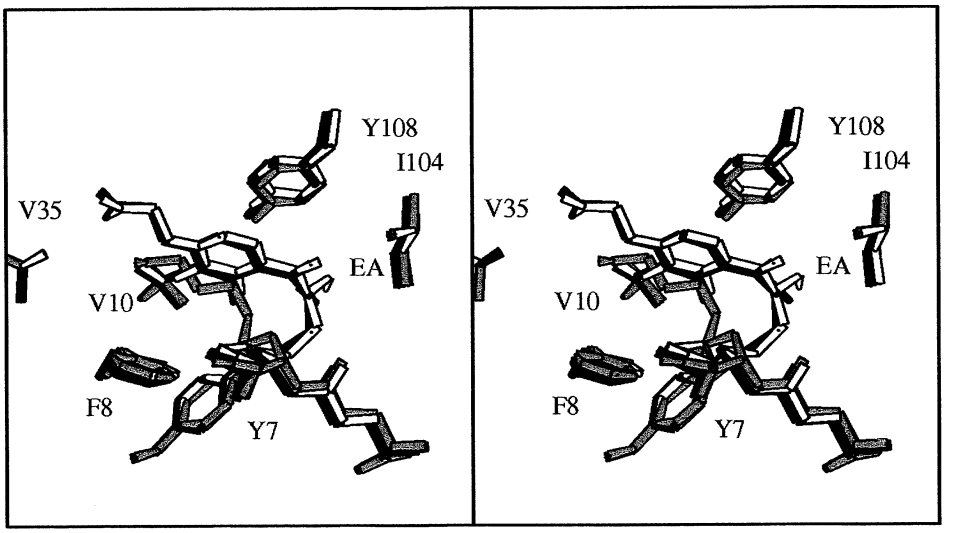

Fig. 3. Superposition of *S*-hexyl GSH and EA-GSH structures in the vicinity of the active site. Filled grey bonds are for the *S*-hexyl GSH complex structure [20], the unfilled bonds represent the EA-GSH complex structure, and the solid black bonds the alternative diastereomer of EA-GSH. The figure was generated with the program MOLSCRIPT [23].

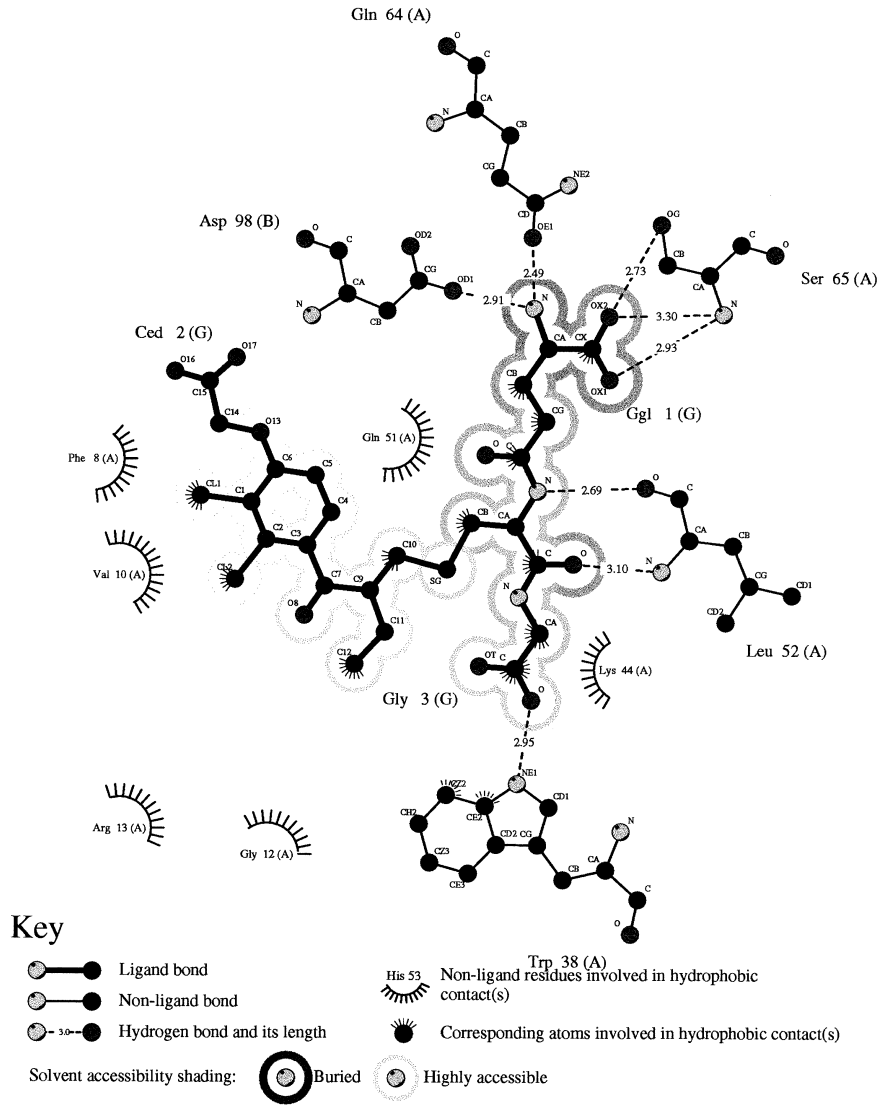

Fig. 4. Schematic drawing of residues that interact with EA-GSH. This figure was produced using the program LIGPLOT [24].

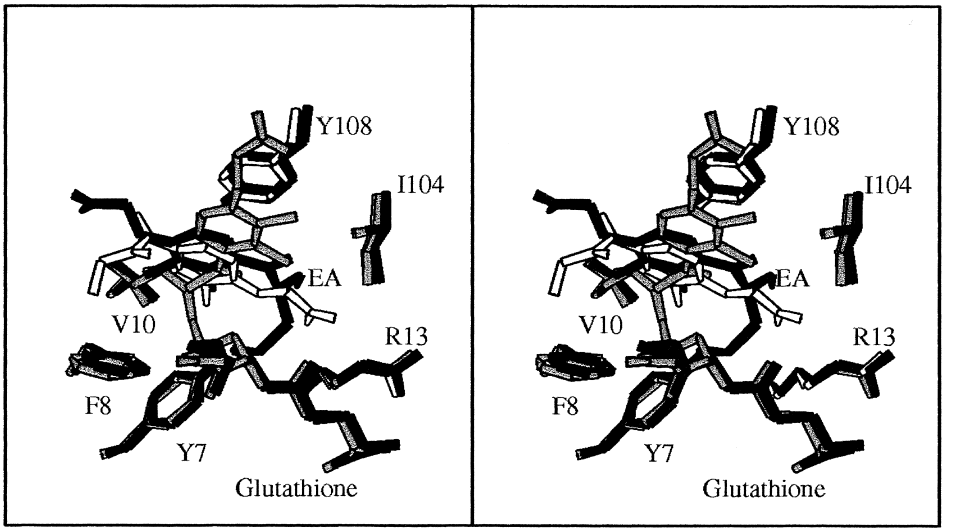

Fig. 5. Superposition of the inhibitor complex structures in the vicinity of the active site. Stippled bonds are for the previously published EA-GSH complex structure [14], hollow bonds for the published EA complex structure [14] and filled bonds are for the EA-GSH complex reported here. The figure was generated with the program MOLSCRIPT [23].

the G site in identical fashion to that previously observed for the GSH moiety of the *S*-hexyl GSH complex. Surprisingly, the aromatic ring of EA was located in a very different position to the position of the hexyl tail in the *S*-hexyl GSH complex and to the position of aromatic ring in the EA complex (Fig. 5). Although still located in the H site, the aromatic ring of EA in the EA-GSH complex was shifted by 2.5 Å and rotated by 120° compared to the aromatic ring in the EA complex. The structure of the human alpha class GST in complex with EA and its glutathione conjugate has recently been published [13]. As expected the aromatic ring of each complex binds in the H site and the GSH moiety binds in the G site. However, it is not straightforward to directly compare the structures of the complexes from the alpha and pi class enzymes since these enzymes exhibit a low pairwise amino acid sequence identity of only 32%. In particular, the H sites are very different due to even lower local sequence identity and to an additional C-terminal helix in the alpha class enzyme that forms part of the H site wall.

The published structures of EA and EA-GSH bound to human pi class GST were based on preformed crystals of wild-type enzyme soaked in inhibitor solutions [14]. The EA-GSH complex presented here is based on crystals which formed by cocrystallisation of enzyme and inhibitor. We observe only one conformation of the inhibitor, unlike the observed binding of EA-GSH to the alpha class enzyme [13]. (In the alpha class enzyme, two conformations were observed in which there was an approximately 140° rotation of the dichlorophenoxy group about the axis defined by the substituents off the C3 and C6 positions of the ring (Fig. 1).) The inhibitor sits in a very similar position to that of the *S*-hexyl GSH in the *S*-hexyl GSH complex structure (Fig. 3) [20]. The GSH moiety of the inhibitor makes essentially identical contacts to residues in the G site of the enzyme as was observed with inhibitor *S*-hexyl GSH [20] and the published EA-GSH structure [14] (Figs. 3 and 4). In total, there are 147 van der Waals interactions (<4 Å), 10 potential hydrogen bonding interactions and three salt bridges between protein and inhibitor (Fig. 4). Superposition of the new EA-GSH complex on the *S*-hexyl GSH complex structure (in the same space group) indicates no significant movement of side-chains in the active site (Fig. 3). The rms deviation in alpha-carbon positions is 0.16 Å, with no deviations greater than 0.5 Å.

The aromatic ring and chlorine atoms of the EA moiety of the EA-GSH complex reported here superimpose very closely to the aromatic ring and chlorine atoms of EA in the crystal structure of the EA complex [14] and there is no significant movement of side-chains within a 15 Å sphere of the active site (Fig. 5). However, the carboxylate moiety now points out into the solvent and the butyryl group forms interactions with Tyr^{108} and Ile^{104} (Figs. 4 and 5). There is a big difference in the location of the aromatic rings between the previously published EA-GSH complex structure [14] and the one reported here. The aromatic rings lie in the same plane but sit adjacent to one another with a shift of about 2.5 Å, and the rings are rotated 120° to each other (Fig. 5). The aromatic ring of the previously published EA-GSH complex forms a parallel stacking interaction with the ring of Tyr^{108} [14] whereas the aromatic ring of the EA-GSH complex reported here is positioned so it optimises packing interactions from the rings of both Tyr^{108} and Phe^{8}. Surprisingly, there is essentially no difference in the number of contacts between inhibitor and protein in either complex (after ignoring water-mediated interactions because the identification of water molecules are, in part, resolution-dependent). Both complexes have a total of 120 protein-inhibitor contacts which include 10 hydrogen bonds and three salt bridges. The origin of the differences between the two complexes is puzzling but is likely related to the fact that in one case the complex was cocrystallised whereas in the other case the inhibitor was soaked into preformed crystals. Both complexes were crystallised at room temperature in the same space group with the same cell dimensions and there are no crystal contacts in the vicinity of the active site in this crystal form. The X-ray diffraction data for both were collected off crystals frozen at 100 K. There was no evidence of the alternative binding mode seen in the elec-

tron density maps of either complex, even when contoured at very low levels (0.3σ).

In the previously published EA-GSH structure there is a water-mediated interaction between the EA ketone oxygen (O8 in Fig. 1) and Tyr^{108} and this suggested a mechanism for the Michael addition of EA to GSH [14]. In the structure here the ketone oxygen is too far away (4.8 Å) from Tyr^{108}. However, the importance of the hydrogen bond for the catalytic mechanism lies in the stereochemistry of the transition state rather than the product so no conclusions can be drawn from these observations.

We have superimposed all the published pi class crystal structures which have GSH conjugates bound. These include the human enzyme in complex with *S*-hexyl GSH [20] and the mouse enzyme in complex with *S*-hexyl GSH and *S*-(*p*-nitrobenzyl) GSH [21]. The result demonstrates that EA [14] and the EA-GSH structure reported here bind in very similar positions to the other inhibitors. The aromatic rings of the EA inhibitors and the nitrobenzyl inhibitor almost superimpose with the rings lying in the same plane but slightly displaced from each other. Thus in both cases the aromatic rings are stacked between the side-chains of Phe^{8} and Tyr^{108}. The EA inhibitors appear to fill the H site better because of the chlorine substituents and in addition there are important van der Waals contacts between the butyryl moieties of the inhibitor and the protein. Just as there is no direct protein interaction with the carboxylate group of the EA-GSH, no interaction was found between the nitro group of the mouse GST inhibitor [21].

The observation that EA-GSH can bind to the pi class GST in different ways reflects the ability of the enzyme to react with a structurally diverse array of substrates. The possibility of multiple modes of ligand binding needs to be taken into account in any structure-based inhibitor design effort on the pi class GST.

Acknowledgements: We gratefully acknowledge financial support from the Anti-Cancer Council of Victoria and the Italian National Research Council ACRO. A.J.O. was the recipient of a National Health and Medical Research Council Postgraduate Research Scholarship and an International Centre for Diffraction Data Crystallography Scholarship. M.W.P. is an Australian Research Council Senior Research Fellow.

References

[1] Coles, B. and Ketterer, B. (1990) CRC Crit. Rev. Biochem. Mol. Biol. 25, 47–70.
[2] Waxman, D.J. (1990) Cancer Res. 50, 6449–6454.
[3] Tsuchida, S. and Sato, K. (1992) CRC Crit. Rev. Biochem. Mol. Biol. 27, 337–384.
[4] Hayes, J.D. and Pulford, D.J. (1995) Crit. Rev. Biochem. Mol. Biol. 30, 445–600.
[5] Ploemen, J.H.T.M., van Ommen, B. and van Bladeren, P.J. (1990) Biochem. Pharmacol. 40, 1631–1635.
[6] Nagourney, R.A., Messenger, J.C., Kern, D.H. and Weisenthal, L.M. (1989) Proc. Am. Assoc. Cancer Res. 30, 574–580.
[7] Hansson, J., Berhane, K., Castro, V.M., Jungnelius, U., Mannervik, B. and Ringborg, U. (1991) Cancer Res. 51, 94–98.
[8] Yang, W.Z., Begleiter, A., Johnston, J.B., Israels, L.G. and Mowat, M.R. (1992) Mol. Pharmacol. 41, 625–630.
[9] O'Dwyer, P.J., LaCreta, F., Nash, S., Tinsley, P.W., Schilder, R., Clapper, M.L., Tew, K.D., Panting, L., Litwin, S., Comis, R.L. and Ozols, R.F. (1991) Cancer Res. 51, 6059–6065.
[10] Phillips, M.F. and Mantle, T.J. (1991) Biochem. J. 275, 703–709.
[11] Awasthi, S., Srivastava, S.K., Ahmad, F., Ahmad, H. and Ansari, G.A.S. (1993) Biochim. Biophys. Acta 1164, 173–178.
[12] Mannervik, B. and Danielson, U.H. (1988) CRC Crit. Rev. Biochem. 23, 283–337.
[13] Cameron, A.D., Sinning, I., L'Hermite, G., Olin, B., Board, P.G., Mannervik, B. and Jones, T.A. (1995) Structure 3, 717–727.
[14] Oakley, A.J., Rossjohn, J., Lo Bello, M., Caccuri, A.M., Federici, G. and Parker, M.W. (1997) Biochemistry 36, 576–585.
[15] Otwinowski, Z. (1993) in: Data Collection and Processing (Sawyer, L., Isaacs, N. and Bailey, S., Eds.), pp. 56–62, SERC Daresbury Laboratory, Warrington.
[16] CCP4 Suite (1994) Acta Crystallogr. D50, 750–763.
[17] Brünger, A.T. (1990) X-PLOR Manual, Yale University, New Haven, CT.
[18] Kleywegt, G. and Jones, T.A. (1994) in: From First Map to Final Model (Bailey, S., Hubbard, R. and Waller, D., Eds.), pp. 59–66, EPSRC, Daresbury Laboratory, Warrington.
[19] Laskowski, R.A., McArthur, M.W., Moss, D.S. and Thorton, J.M. (1993) J. Appl. Crystallogr. 26, 282–291.
[20] Reinemer, P., Dirr, H.W., Ladenstein, R., Huber, R., Lo Bello, M., Federici, G. and Parker, M.W. (1992) J. Mol. Biol. 227, 214–226.
[21] García-Sáez, I., Párraga, A., Phillips, M.F., Mantle, T.J. and Coll, M. (1994) J. Mol. Biol. 237, 298–314.
[22] Lamotte, P.J., Campsteyn, H., Dupont, L. and Vermeire, M. (1978) Acta Crystallogr. B34, 2636–2638.
[23] Kraulis, P. (1991) J. Appl. Crystallogr. 24, 946–950.
[24] Wallace, A.C., Laskowski, R.A. and Thornton, J.M. (1995) Protein Eng. 8, 127–134.